

J/ψ Polarization at Hadron Colliders in Nonrelativistic QCD

Kuang-Ta Chao,^{1,2} Yan-Qing Ma,^{1,3} Hua-Sheng Shao,¹ Kai Wang,¹ and Yu-Jie Zhang⁴

¹*Department of Physics and State Key Laboratory of Nuclear Physics and Technology, Peking University, Beijing 100871, China*

²*Center for High Energy Physics, Peking University, Beijing 100871, China*

³*Physics Department, Brookhaven National Laboratory, Upton, New York 11973, USA*

⁴*Key Laboratory of Micro-nano Measurement-Manipulation and Physics (Ministry of Education) and School of Physics, Beihang University, Beijing 100191, China*

(Received 14 January 2012; published 15 June 2012)

With nonrelativistic QCD factorization, we present a full next-to-leading order computation of the polarization observable for J/ψ production at hadron colliders including all important Fock states, i.e., $^3S_1^{[1,8]}$, $^1S_0^{[8]}$, and $^3P_J^{[8]}$. We find the $^3P_J^{[8]}$ channel contributes a positive longitudinal component and a negative transverse component, so the J/ψ polarization puzzle may be understood as the transverse components canceling between the $^3S_1^{[8]}$ and $^3P_J^{[8]}$ channels, which results in mainly the unpolarized (even slightly longitudinally polarized) J/ψ . This may give a possible solution to the long-standing J/ψ polarization puzzle. Predictions for J/ψ polarization at the LHC are also presented.

DOI: 10.1103/PhysRevLett.108.242004

PACS numbers: 12.38.Bx, 13.60.Le, 13.88.+e, 14.40.Pq

Nonrelativistic QCD (NRQCD) [1] is an effective field theory approach for heavy quarkonium. At present, one of the main obstacles to NRQCD is the polarization puzzle of J/ψ hadroproduction [2]. At leading order (LO) in α_s , J/ψ production is dominated by gluon fragmentation to a color-octet (CO) $^3S_1^{[8]} c\bar{c}$ pair at high transverse momentum p_T , which leads to the transversely polarized J/ψ [3]. But the CDF Collaboration found the prompt J/ψ in its helicity frame to be unpolarized and even slightly longitudinally polarized [4]. Despite numerous attempts made in the past, the puzzle still remains.

For unpolarized J/ψ production, important progress has been made in recent years. It was found that the next-to-leading order (NLO) QCD corrections to differential cross sections of the $^3S_1^{[1]}$ channel can be as large as 2 orders of magnitude at high p_T [5], while those of the $^1S_0^{[8]}$ and $^3S_1^{[8]}$ channels are small [6]. Furthermore, NLO corrections of the $^3P_J^{[1]}$ [7] and $^3P_J^{[8]}$ [8,9] channels are found to also be very large. These large corrections are well understood because at NLO the differential cross section $d\sigma/dp_T$ receives contributions from new topologies that scale with p_T in a different manner from the LO calculation. By including NLO corrections, one may explain the existing unpolarized cross sections of p_T up to 70 GeV [7,8].

Accordingly, it is necessary to examine the J/ψ polarization at NLO. Among various channels, the correction to J/ψ polarization via the $^3S_1^{[1]}$ channel was worked out in Ref. [10], which alters the polarization from being transverse at LO to longitudinal at NLO. This phenomenon was explained recently in collinear factorization [11] as next-to-leading power dominance. As for the $^3S_1^{[8]}$ channel, the NLO correction can only slightly change the polarization [6], while the $^1S_0^{[8]}$ channel gives an unpolarized result to all orders in α_s . As a result, up to date theoretical

predictions may indicate a serious puzzle for J/ψ polarization [6]. However, the NLO correction of the $^3P_J^{[8]}$ channel to J/ψ polarization has not been calculated. In this Letter, we perform this calculation and show that the NLO contribution of the $^3P_J^{[8]}$ channel is indeed crucial in clarifying the long-standing J/ψ polarization puzzle in NRQCD.

We first introduce some formalisms in our calculation. The J/ψ can decay into an easily identified lepton pair. The information about the J/ψ polarization is encoded in the angular distributions of the leptons. The two-body leptonic decay angular distribution of the J/ψ in its rest frame is usually parametrized as [12]

$$\frac{d\mathcal{N}}{d\cos\theta} \propto 1 + \lambda_\theta \cos^2\theta, \quad \lambda_\theta = \frac{d\sigma_{11} - d\sigma_{00}}{d\sigma_{11} + d\sigma_{00}}. \quad (1)$$

Here, $d\sigma_{ij}$ ($i, j = 0, \pm 1$, with respect to the z components of J/ψ) represents the ij contribution in the spin density matrix formalism. In the literature, the polarization observable λ_θ is also denoted as $\alpha = \frac{d\sigma_T - 2d\sigma_L}{d\sigma_T + 2d\sigma_L}$. The differential cross sections are

$$d\sigma_{s_z s_z} = \sum_{ijn} \int dx_1 dx_2 f_{i/H_1}(x_1, \mu_F) \times f_{j/H_2}(x_2, \mu_F) \langle \mathcal{O}_n \rangle d\hat{\sigma}_{s_z s_z}^{ij,n}, \quad (2)$$

where the $\langle \mathcal{O}_n \rangle$ are the long-distance matrix elements (LDMEs) for $n = ^3S_1^{[1,8]}$, $^3P_J^{[8]}$, and $^1S_0^{[8]}$. In general, the partonic cross sections $d\hat{\sigma}_{s_z s_z}^{ij,n}$ can be obtained from the spin density matrix elements [12]

$$\rho_{s_z s_z} \{ij \rightarrow (c\bar{c})[n]X\} \propto \sum_{L_z} |\mathcal{M}\{ij \rightarrow (c\bar{c})[L_z, s_z]X\}|^2. \quad (3)$$

In practice, several polarization frame definitions have been used in the literature. In the s -channel helicity frame, the polar axis is chosen as the flight direction of the J/ψ in the laboratory frame. Another frequently used frame is the so-called Collins-Soper frame [13]. For simplicity, here we will only choose the helicity frame, the same as used by CDF [4]. The full theoretical predictions of azimuthal correlations and the theoretical descriptions by Collins-Soper, and feed down from χ_{cJ} and ψ' will be presented in a forthcoming publication.

We describe our method briefly for the sake of completeness. Some improvements are made in our calculations, while most of our method has been encompassed in Ref. [8]. The calculations of real corrections are based on the Dyson-Schwinger equations. After absorbing the core codes of the published HELAC [14], we promote it into a form that can generate the matrix element of heavy quarkonia (especially P -wave) production at colliders by adding some P -wave off-shell currents. The virtual corrections are treated analytically, and the helicity matrix elements are obtained using the spinor helicity method [15].

For numerical results, we choose the same input parameters as in Ref. [8]. Specifically, the renormalization scale μ_r , factorization scale μ_f , and NRQCD scale μ_Λ are chosen as $\mu_r = \mu_f = m_T = \sqrt{4m_c^2 + p_T^2}$ and $\mu_\Lambda = m_c$. Scale dependence is estimated by varying μ_r , μ_f , by a factor of $\frac{1}{2}$ to 2 with respect to their central values. By fitting only the cross sections, it was found that only two linear combinations of the CO LDMEs can be extracted [8]. Since polarization information is also available, we will try to extract the three independent CO LDMEs using the polarization observable λ_θ and the production rate $d\sigma/dp_T$ of the J/ψ measured by CDF Run II [4] simultaneously, where the data in the low transverse momentum region ($p_T < 7$ GeV) are not included in our fit because of existing nonperturbative effects. By minimizing χ^2 , the CO LDMEs are obtained and listed in the first row of Table I. In Fig. 1, we compare λ_θ from the Tevatron data with our theoretical results.

To understand the unpolarized results, λ_θ for each channel is drawn in Fig. 2, where for the NLO ${}^3P_J^{[8]}$ channel we mean the value of $(d\hat{\sigma}_{11} - d\hat{\sigma}_{00})/|d\hat{\sigma}_{11} + d\hat{\sigma}_{00}|$ because $d\hat{\sigma}_{11} + d\hat{\sigma}_{00}$ decreases from being positive to negative as p_T increases. In addition to the known polarization of the S -wave [6,10], the ${}^3P_J^{[8]}$ channel satisfies $(d\hat{\sigma}_{11} - d\hat{\sigma}_{00})/|d\hat{\sigma}_{11} + d\hat{\sigma}_{00}| < -1$ in our considered p_T region, which results from $d\hat{\sigma}_{11} < 0$ and $d\hat{\sigma}_{00} > 0$. Therefore, the transverse component of ${}^3P_J^{[8]}$ is negative, which effectively gives a longitudinal contribution to λ_θ , and the longitudinal component of ${}^3P_J^{[8]}$ is positive. In some of the parameter space of the CO LDMEs, the positive transverse component of ${}^3S_1^{[8]}$ will largely be canceled by the negative transverse component of ${}^3P_J^{[8]}$, which yields a small

TABLE I. Different sets of CO LDMEs for the J/ψ . Values in the first row are obtained by fitting the differential cross section and polarization of the prompt J/ψ simultaneously at the Tevatron [4]. Values in the second and third rows are two extreme choices for these CO LDMEs. The color-singlet LDME is calculated by the B - T potential model in [16].

$\langle \mathcal{O}({}^3S_1^{[1]}) \rangle$	$\langle \mathcal{O}({}^1S_0^{[8]}) \rangle$	$\langle \mathcal{O}({}^3S_1^{[8]}) \rangle$	$\langle \mathcal{O}({}^3P_0^{[8]}) \rangle / m_c^2$
GeV ³	10 ⁻² GeV ³	10 ⁻² GeV ³	10 ⁻² GeV ³
1.16	8.9 ± 0.98	0.30 ± 0.12	0.56 ± 0.21
1.16	0	1.4	2.4
1.16	11	0	0

transverse component and results in an unpolarized or even longitudinal λ_θ . This explains why the complete NLO calculation gives an unpolarized prediction in Fig. 1.

It is interesting to see that, by choosing the proper CO LDMEs, complete NLO predictions in NRQCD factorization can be made compatible with the data. This is distinct from all previous NRQCD predictions that give strong transverse polarizations for the J/ψ [2]. Furthermore, we want to emphasize the following four points.

(1) Transverse components with large cancellation between ${}^3S_1^{[8]}$ and ${}^3P_J^{[8]}$ determine a specific parameter space for the CO LDMEs. Using the same treatment as in Ref. [8], we decompose the transverse component of the short-distance coefficient of ${}^3P_J^{[8]}$ into a linear combination of ${}^3S_1^{[8]}$ and ${}^1S_0^{[8]}$ as $d\hat{\sigma}_{11}({}^3P_J^{[8]}) = 2.47d\hat{\sigma}_{11}({}^1S_0^{[8]}) - 0.52d\hat{\sigma}_{11}({}^3S_1^{[8]})$. Since $d\hat{\sigma}_{11}({}^1S_0^{[8]}) \ll d\hat{\sigma}_{11}({}^3S_1^{[8]})$ when $p_T > 7$ GeV, the cancellation requirement is approximately equivalent to the absence of the linear combination $\langle \mathcal{O}({}^3S_1^{[8]}) \rangle - 0.52\langle \mathcal{O}({}^3P_J^{[8]}) \rangle / m_c^2$, which is close to $M_1 = \langle \mathcal{O}({}^3S_1^{[8]}) \rangle - 0.56\langle \mathcal{O}({}^3P_J^{[8]}) \rangle / m_c^2$ defined in Ref. [8]. Recall that to have a good fit for the unpolarized yield one needs a very small M_1 , so the conditions for the CO LDMEs parameter space introduced by fitting

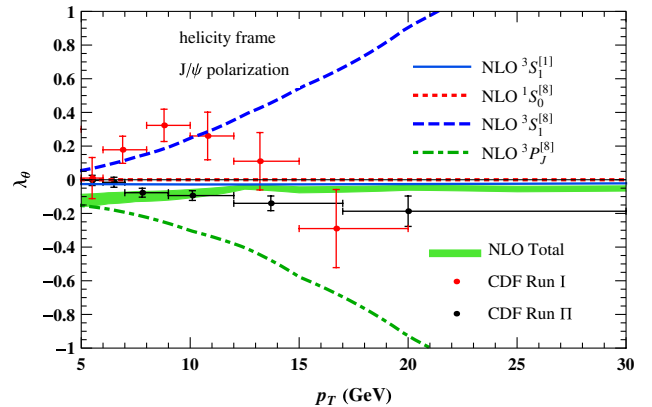


FIG. 1 (color online). NLO results for the polarization observable λ_θ of J/ψ production at the Tevatron. The CDF experimental data are taken from Ref. [4].

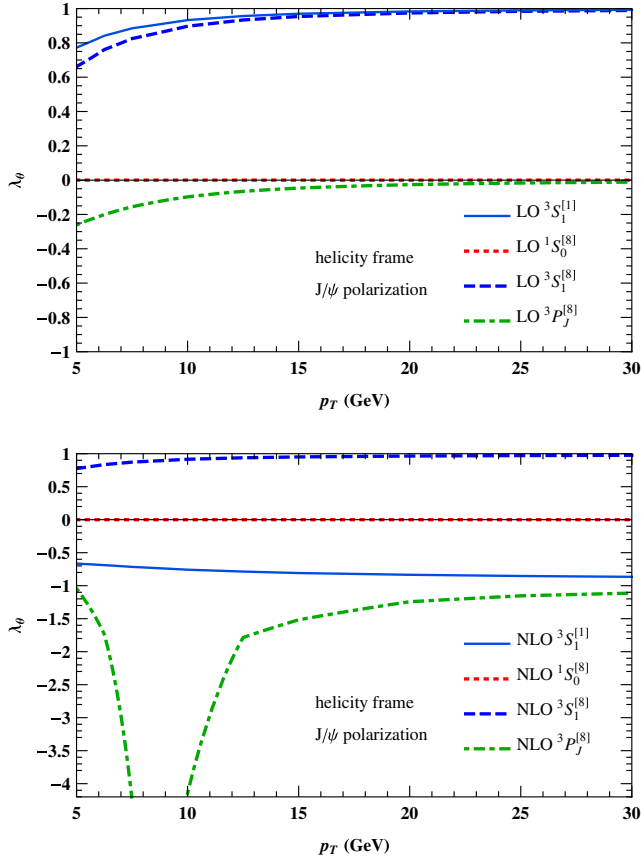


FIG. 2 (color online). The p_T dependence of λ_θ for ${}^3S_1^{[11]}$, ${}^1S_0^{[8]}$, ${}^3S_1^{[8]}$, and ${}^3P_J^{[8]}$ channels with $\sqrt{s} = 1.96$ TeV and $|y_{J/\psi}| < 0.6$. For the NLO ${}^3P_J^{[8]}$ channel, the curve corresponds to the value of $(d\hat{\sigma}_{11} - d\hat{\sigma}_{00})/|d\hat{\sigma}_{11} + d\hat{\sigma}_{00}|$.

both yield and polarization are consistent with each other. Good agreement with the LHC data for the J/ψ cross sections can be found in Fig. 3 using the LDMEs in Table I.

(2) As the yield and polarization share a common parameter space, and the yield can only constrain two linear combinations of CO LDMEs, the combined fit of both yield and polarization may also not constrain three independent CO LDMEs stringently. In fact we find for a wide range of given $\langle\mathcal{O}({}^1S_0^{[8]})\rangle$, one can fit both yield and polarization reasonably well. The CO LDMEs under two extreme conditions are listed in Table I. When $\langle\mathcal{O}({}^1S_0^{[8]})\rangle$ is chosen to be its maximal value, the J/ψ is unpolarized; when $\langle\mathcal{O}({}^1S_0^{[8]})\rangle$ vanishes, λ_θ increases from -0.25 at $p_T = 5$ GeV to 0 at $p_T = 15$ GeV at the Tevatron. Even in these two extreme cases, the theoretical predictions of the J/ψ cross section and polarization are still close to the Tevatron data, and are also consistent with the observed cross sections obtained by ATLAS [17] and CMS [18] at the LHC as shown in Fig. 3. As a result, although it is hard to determine the CO LDMEs precisely, we find that the polarization puzzle can be much eased for a wide range of $\langle\mathcal{O}({}^1S_0^{[8]})\rangle$ values.

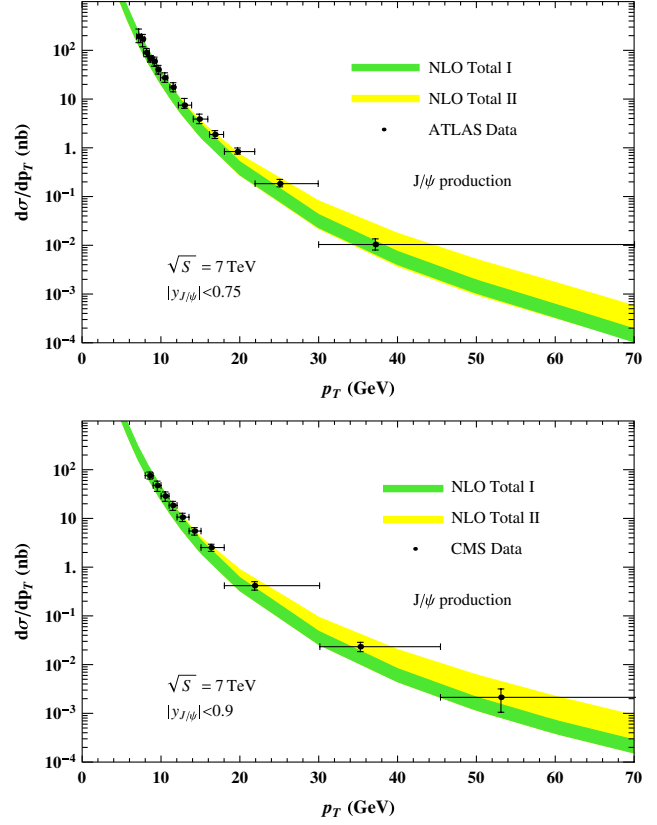


FIG. 3 (color online). Cross sections of J/ψ production at the LHC with the LDMEs shown in Table I. The darker bands (NLO Total I) correspond to the LDMEs in the first row of Table I. The lighter bands (NLO Total II) correspond to the LDMEs in the second row [$\langle\mathcal{O}({}^1S_0^{[8]})\rangle = 0$ (upper bounds)] and third row [$\langle\mathcal{O}({}^3S_1^{[8]})\rangle = \langle\mathcal{O}({}^3P_J^{[8]})\rangle = 0$ (lower bounds)] of Table I. The ATLAS data are taken from Ref. [17], and the CMS data from Ref. [18].

(3) The cancellation of the transverse component between the ${}^3S_1^{[8]}$ and ${}^3P_J^{[8]}$ channels is not problematic, since the contribution of an individual channel is unphysical and depends on the renormalization scheme and scale [8]. A “physical” requirement is that the summation $d\sigma_{11}({}^3S_1^{[8]} + {}^3P_J^{[8]})$ be positive, which is satisfied in the fit.

(4) It is important to note that the LDMEs presented here are significantly different from those extracted from the global fit in Ref. [19]. As hadroproduction data play the most important role in Ref. [19], this difference cannot be mainly attributed to data other than hadroproduction not being considered in our fit. In fact, one can track to the situation where only hadroproduction data are used in the global fit. As explained in Ref. [8], our choice of the p_T cut for the hadroproduction data is $p_T > 7$ GeV while the cut in Ref. [19] is $p_T > 3$ GeV, and our LDMEs can well describe the produced p_T distribution in the region $7 \text{ GeV} < p_T < 70 \text{ GeV}$ (see Fig. 3), while the fit in Ref. [19] puts stress on the smaller p_T region and gives too smooth a p_T distribution at large p_T . This is the main

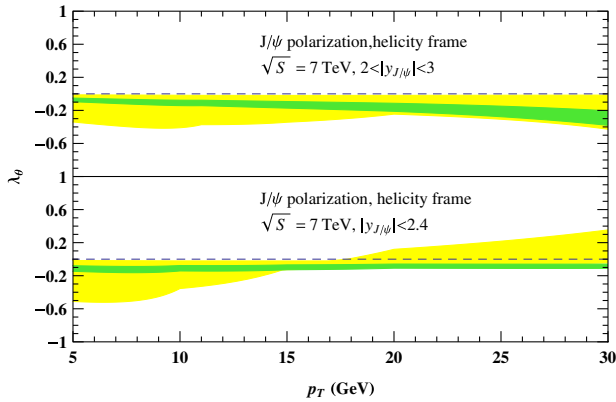


FIG. 4 (color online). NLO predictions of the J/ψ polarization observable λ_θ at the LHC. The uncertainty is shown by large lighter bands when varying the CO LDME $\langle\mathcal{O}(^1S_0^{[8]})\rangle$. The bounds of $\lambda_\theta = 0$ in the lighter bands correspond to CO LDMEs in the third row of Table I, while the other bounds correspond to the second row of Table I. The small darker bands are the predictions using the CO LDMEs in the first row of Table I.

reason why our LDMEs differ from those in Ref. [19]. In our view, for the small p_T region the fixed order perturbation calculation may need to be modified by considering soft gluon emission and other nonperturbative effects. We see that the two treatments in Ref. [8] and Ref. [19] have different features and should be tested by more experiments in the future.

There are still other uncertainties, such as the charm quark mass, but they do not change the qualitative properties of our result. Predictions of the polarization observable λ_θ at the LHC with $\sqrt{S} = 7$ TeV are plotted in Fig. 4, where only the forward region ($2 < |y_{J/\psi}| < 3$) and the central region ($|y_{J/\psi}| < 2.4$) are considered. [Note that the ALICE Collaboration has measured J/ψ polarization recently with rapidity $2.5 < |y_{J/\psi}| < 4$ [20]. But the measured transverse momenta ($2 \text{ GeV} < p_T < 8 \text{ GeV}$) are smaller than considered in this Letter.] The large error bar (lighter bands) in these predictions is caused by a lack of knowledge of $\langle\mathcal{O}(^1S_0^{[8]})\rangle$; thus, we scan all its possible values in the predictions. It is found in these predictions that λ_θ becomes sensitive to $\langle\mathcal{O}(^1S_0^{[8]})\rangle$ when $p_T > 20$ GeV, so it may be possible to extract three independent CO LDMEs when polarization data at high p_T are available.

In summary, we present a full NLO calculation including $^3S_1^{[1]}$, $^3S_1^{[8]}$, $^1S_0^{[8]}$, and $^3P_J^{[8]}$ for the polarization observable λ_θ of the J/ψ in the helicity frame at the Tevatron and LHC. Results of S -wave channels are consistent with those in the literature [10], while those of the $^3P_J^{[8]}$ channel are new and play a crucial role in understanding the polarization puzzle. Our calculation shows that the transverse component of the $^3P_J^{[8]}$ channel is negative, while its

longitudinal component is positive. Thus the $^3P_J^{[8]}$ channel gives a maximal longitudinal contribution. By choosing suitable CO LDMEs, which bring about good agreement with the observed J/ψ cross sections at large p_T at the LHC, the transverse components can be largely canceled between the $^3S_1^{[8]}$ and $^3P_J^{[8]}$ channels, leaving the remaining terms to be dominated by the unpolarized J/ψ . This may give a possible solution to the long-standing J/ψ polarization puzzle within NRQCD factorization. Although it is hard to individually extract the three independent CO LDMEs in an accurate way, our interpretation of J/ψ polarization makes sense by using only their combinations. We also present polarization predictions for the LHC.

We thank C. Meng for helpful discussions. This work was supported in part by the National Natural Science Foundation of China (Grants No. 11021092, No. 11075002, and No. 11075011), and the Ministry of Science and Technology of China (2009CB825200). Y. Q. M. is also supported by the U.S. Department of Energy, Contract No. DE-AC02-98CH10886.

Note added.—When this Letter was being prepared, a preprint [21] on the same issue had just appeared. The essential difference is that they have a negative $\langle\mathcal{O}(^3P_0^{[8]})\rangle$ based on a global fit [19], and give a significant transverse polarization prediction, but our fit leads to a positive $\langle\mathcal{O}(^3P_0^{[8]})\rangle$, which is consistent with the observed cross sections in a wide p_T region (7–70 GeV) at the LHC, and results in the mainly unpolarized J/ψ .

-
- [1] G. T. Bodwin, E. Braaten, and G. P. Lepage, *Phys. Rev. D* **51**, 1125 (1995); **55**, 5853(E) (1997).
 - [2] N. Brambilla *et al.*, *Eur. Phys. J. C* **71**, 1534 (2011).
 - [3] E. Braaten, B. A. Kniehl, and J. Lee, *Phys. Rev. D* **62**, 094005 (2000).
 - [4] T. Affolder *et al.* (CDF Collaboration), *Phys. Rev. Lett.* **85**, 2886 (2000). A. Abulencia *et al.* (CDF Collaboration), *Phys. Rev. Lett.* **99**, 132001 (2007).
 - [5] J. M. Campbell, F. Maltoni, and F. Tramontano, *Phys. Rev. Lett.* **98**, 252002 (2007).
 - [6] B. Gong, X. Q. Li, and J.-X. Wang, *Phys. Lett. B* **673**, 197 (2009); **693**, 612(E) (2010).
 - [7] Y.-Q. Ma, K. Wang, and K.-T. Chao, *Phys. Rev. D* **83**, 111503 (2011).
 - [8] Y.-Q. Ma, K. Wang, and K.-T. Chao, *Phys. Rev. Lett.* **106**, 042002 (2011). Y.-Q. Ma, K. Wang, and K.-T. Chao, *Phys. Rev. D* **84**, 114001 (2011).
 - [9] M. Butenschön and B. A. Kniehl, *Phys. Rev. Lett.* **106**, 022003 (2011).
 - [10] B. Gong and J.-X. Wang, *Phys. Rev. Lett.* **100**, 232001 (2008).
 - [11] Z.-B. Kang, J.-W. Qiu, and G. Sterman, *Phys. Rev. Lett.* **108**, 102002 (2012).
 - [12] M. Noman and S. D. Rindani, *Phys. Rev. D* **19**, 207 (1979); M. Beneke, M. Kramer, and M. Vanttinen, *Phys. Rev. D* **57**, 4258 (1998).

-
- [13] J.C. Collins and D.E. Soper, *Phys. Rev. D* **16**, 2219 (1977).
- [14] A. Cafarella, C. G. Papadopoulos, and M. Worek, *Comput. Phys. Commun.* **180**, 1941 (2009).
- [15] R. Kleiss and W.J. Stirling, *Nucl. Phys.* **B262**, 235 (1985).
- [16] E.J. Eichten and C. Quigg, *Phys. Rev. D* **52**, 1726 (1995).
- [17] G. Aad *et al.* (ATLAS Collaboration), *Nucl. Phys.* **B850**, 387 (2011).
- [18] S. Chatrchyan *et al.* (CMS Collaboration), *J. High Energy Phys.* **02**, (2012) 011.
- [19] M. Butenschön and B. A. Kniehl, *Phys. Rev. D* **84**, 051501 (2011).
- [20] B. Abelev *et al.* (ALICE Collaboration), *Phys. Rev. Lett.* **108**, 082001 (2012).
- [21] M. Butenschön and B. A. Kniehl, *Phys. Rev. Lett.* **108**, 172002 (2012).